This is a repository copy of *Zinc 1s Valence-to-Core X-ray Emission Spectroscopy of Halozincate Complexes*.

White Rose Research Online URL for this paper:
http://eprints.whiterose.ac.uk/152683/

Version: Accepted Version

Zinc 1s Valence-to-Core X-Ray Emission Spectroscopy of Halozincate Complexes

Coby J. Clarke,[†] Shusaku Hayama,[‡] Alexander Hawes,[¶] Jason P. Hallett,[†]
Thomas W. Chamberlain,[¶] Kevin R. J. Lovelock,[*,§] and Nicholas A. Besley[*,∥]

†*Department of Chemical Engineering, Imperial College, London, SW7 2AZ, UK*

‡*Diamond Light Source, Didcot, Oxfordshire, OX11 0DE, UK*

¶*Institute of Process Research and Development, School of Chemistry, University of Leeds,
LS2 9JT, UK*

§*Department of Chemistry, University of Reading, Reading, RG6 6AD, UK.*

∥*School of Chemistry, University of Nottingham, University Park, Nottingham, NG7 2RD,
UK.*

E-mail: k.r.j.lovelock@reading.ac.uk; nick.besley@nottingham.ac.uk

Abstract

The Zn 1s valence-to-core (VtC) X-ray emission spectra of seven ionic liquids
have been measured experimentally and simulated based upon time-dependent density-
functional theory (TDDFT) calculations. Six of the ionic liquids were made by mixing
$[C_8C_1Im]X$ and $Zn(II)X_2$ at three different ZnX_2 mole fractions (0.33, 0.50 or 0.67) for
X=Cl or Br, and a further ionic liquid was made by mixing $[P_{6,6,6,14}]Cl$ and a mole
fraction of $ZnCl_2$ of 0.33. Calculations were performed for the $[ZnX_4]^{2-}$, $[Zn_2X_6]^{2-}$ and
$[Zn_4X_{10}]^{2-}$ ions to capture the expected metal complex speciation. The VtC emission
spectra showed three bands arising from single electron processes that can be assigned
to emission from ligand p-type orbitals, zinc d orbitals and ligand s-type orbitals. For

1

all seven ionic liquids, the highest occupied molecular orbital arises from the ligand p orbitals, and the spectra for the different size metal complexes for the same X were found to be very similar, in terms of both relative peak intensities and peak energies. For both experiments and TDDFT calculations, there was an energy difference of 0.5 eV between the Cl-based and Br-based metal complexes for the ligand s and p orbitals, while the Zn 3d orbital energies were relatively unaffected by the identity of the ligand. The TDDFT calculations find that for the ions with symmetrically equivalent zinc atoms ($[Zn_2X_6]^{2-}$ and $[Zn_4X_{10}]^{2-}$), the most appropriate core-ionised reference state has a core-hole that is localised on a single zinc atom. In this framework, the spectra for the larger ions can be viewed as a sum of spectra for the tetrahedral complex with a single zinc atom with small variations in the structure of the coordinating ligands. Since the spectra are relatively insensitive to small changes in the geometry of the ligands, this is consistent with the small variation in the spectra measured in experiment.

Introduction

X-ray emission spectroscopy (XES) has become established as a powerful technique to probe the electronic structure of molecular systems.[1–3] XES probes the occupied molecular orbitals and is complementary to X-ray absorption spectroscopy (XAS) which is sensitive to the unoccupied orbitals. One advantage of these techniques is that they provide an element specific, local probe of geometric and electronic structure. In recent years, the development of new light sources has greatly expanded the breadth of systems that can be studied using X-ray spectroscopy. One example of this is the XES of transition metal complexes at the metal K-edge, i.e. following the non-resonant ionisation of the metal 1s electron.

The most prominent features in the metal K-edge XES of transition metal complexes are the K_α and $K\beta_{1,3}$ emission lines arising from electric dipole allowed metal 2p→1s and 3p→1s

transitions, respectively.[4] However, there is greater interest in much weaker transitions that occur at higher energies. This region of the spectrum is referred to as the valence-to-core (VtC) region and comprises transitions from orbitals associated with the ligands. This region has two groups of features, the $K\beta''$ lines that arise from ligand-valence s→metal 1s transitions and the $K\beta_{2,5}$ lines corresponding to ligand-valence p→metal 1s transitions. The reason for the focus on the VtC region is that these transitions can provide information on the nature of the metal-ligand bonding.[5] A number of systems have been studied including iron, chromium, vanadium, manganese and zinc complexes,[4,6–17] and XES has also been used to probe the structure of enzymes.[18]

Halozincate ionic liquids show promise as mild Lewis acid catalysts.[19–23] The ability to tune the Lewis acidity by changing the mole fraction of ZnX_2 used to make the ionic liquid gives major advantages, but understanding the physicochemical properties of different halozincate metal complexes is in its infancy. In addition, halozincate ionic liquids are excellent model systems for understanding the electronic structure of metal complexes in solution. The speciation of halozincate ionic liquids is relatively well understood. At a ZnX_2 mole fraction of x = 0.33, the only metal complex will be $[ZnCl_4]^{2-}$.[24] At x = 0.50 and x = 0.67, the expected metal complexes are $[Zn_2Cl_6]^{2-}$ and $[Zn_4Cl_{10}]^{2-}$ respectively,[25] although the presence of low concentrations of other halozincate metal complexes is possible.

Alongside the development of experimental measurements, there has also been advances in the simulation of XES. The energy and matrix elements of the electric dipole moment operator for the various valence to core transitions required to simulate an X-ray emission spectrum can be evaluated directly from wavefunction[26–29] or Kohn-Sham density functional theory (DFT)[30] calculations. For example, the excitation energy can be determined from the energy difference between the orbital energies (ϵ_i)

$$\Delta E = \epsilon_v - \epsilon_c \qquad (1)$$

and the oscillator strength estimated from

$$f \propto |\langle \phi_c | \hat{\mu} | \phi_v \rangle|^2 \qquad (2)$$

where ϕ_c is a core orbital with energy ϵ_c and ϕ_v is a valence orbital with energy ϵ_v, and this and related approaches have been applied to study transition metal complexes.[4,31] Following ionisation of a core electron there will be some relaxation of the electronic structure. This can be included in the calculations through the use of the Z+1 approximation where an increased nuclear charge is used for the absorbing atom[6] or through the transition potential approach where a half filled core orbital is used providing a balance between final and initial states.[32] The relaxation of the electronic structure in the presence of the core-hole can be included explicitly in the calculations through a Δself-consistent field (SCF) approach wherein separate SCF calculations are performed for each state.[33] However, this approach can be cumbersome since individual SCF calculations are necessary for all of the relevant states. Alternatively, XES spectra can be determined from conventional response theory calculations through the use of a reference determinant with a core-hole and the transitions of interest are found as those with negative eigenvalues.[34] In this approach full relaxation of the orbitals in the presence of the core-hole is included in the ionised state. This was originally applied within the context of equation-of-motion coupled cluster theory (EOM-CCSD)[35] and time-dependent density functional theory (TDDFT)[36,37] and has recently been applied within the context of the algebraic construction (ADC) methods.[38] The XES of transition metal systems has been studied using TDDFT,[17,39,40] and it has been shown that the experimental spectra are reproduced well although an energy shift needs to be applied to the calculated spectra to align with experiment owing to deficiencies in the exchange-correlation functional associated with the electron self-interaction error.[36]

Another important factor for these calculations is the choice of gaussian basis set.[41] The effective nuclear charge of the core-ionised state increases by one leading to a contraction of the electron density, which presents a challenge for the basis set to describe both ground and core-ionised states equally well. This can be achieved through the use of large Dunning basis sets with core-correlation functionals, such as cc-pCVTZ and cc-pCVQZ.[40] Recently, alternative strategies have emerged for achieving a balanced description of both states. These include using exponents for the basis functions midway between the element and the element with a nuclear charge of one higher[42] and explicitly including basis functions for the Z+1 element in the basis set.[43]

In this paper we present experimental measurements and calculations of the XES of seven halozincate ionic liquids, which were made by mixing $[C_8C_1Im]X$ and $Zn(II)X_2$ at three different ZnX_2 mole fractions (0.33, 0.50 or 0.67) and with two different X (Cl or Br), and a further ionic liquid was made by mixing $[P_{6,6,6,14}]Cl$ and a mole fraction of $ZnCl_2$ of 0.33. Calculations were performed for the $[ZnX_4]^{2-}$, $[Zn_2X_6]^{2-}$ and $[Zn_4X_{10}]^{2-}$ ions to capture the expected metal complex speciation. The VtC X-ray emission spectra were recorded for six halozincate ionic liquids and compared with spectra computed with DFT and TDDFT. The series of zinc complexes studied allows the capability of the calculations to reproduce subtle differences in the spectra to be studied. The majority of studies on VtC XES have focused on metal complexes with a single metal centre. The XES of oxo-bridged iron complexes[11] and manganese complexes[9] has been studied, and it was found that the intensity of the features was dependent on the bond angle in addition to the metal-ligand bond distance.[11] The complexes studied here have multiple zinc atoms (up to four) and their symmetrical nature raises additional questions with regard to the nature of the core hole upon the ionisation of a zinc 1s electron. More specifically, whether the core-hole is localised on a single zinc atom or delocalised over more than one zinc atom.

Experimental Methods

1-Octyl-3-methylimidazolium chloride, $[C_8C_1Im]Cl$, and 1-octyl-3-methylimidazolium bromide, $[C_8C_1Im]Br$, ($\approx$250 g ea.) were purchased from Iolitec and tetradecyl(trihexyl)phosphonium chloride, $[P_{6,6,6,14}]Cl$, was purchased from Sigma-Aldrich. They were dried on a Schlenk line at $<$2x10^{-2} mbar at 70 °C for 48 hr before being transferred to a LABstar (MBraun) glovebox with $<$0.5 ppm O_2 and H_2O. The viscous ionic liquids were gently heated to 40 °C and 2 - 3 g of ionic liquid was decanted into a series of 30 ml screw top glass vials and the masses were recorded. The desired amount of ZnX_2 ($ZnCl_2$ and $ZnBr_2$ both purchased from Sigma-Aldrich, purity 99.999% metals basis, used as received) was calculated and weighed in to each vial, stirrer bars were added, and the temperature was raised to 70 °C. The vials were periodically handled to wash any solid particles from the sides until clear solutions persisted (typically $<$48 hr).

Table 1: Synthesis of halozincate ionic liquids. x = 0.33 $\Rightarrow$ 2$[C_8C_1Im]X$ + ZnX_2 $\rightarrow$ $[C_8C_1Im]_2[ZnX_4]$; x = 0.50 $\Rightarrow$ 2$[C_8C_1Im]X$ + 2ZnX_2 $\rightarrow$ $[C_8C_1Im]_2[Zn_2X_6]$; x = 0.67 $\Rightarrow$ 2$[C_8C_1Im]X$ + 4ZnX_2 $\rightarrow$ $[C_8C_1Im]_2[Zn_4X_{10}]$

Ionic Liquid	X	Desired Mole Fraction ZnX_2, x	Mass Ionic Liquid / g	Moles Ionic Liquid / mmol	Mass ZnX_2 / g	Moles ZnX_2 /mmol	Actual Mole Fraction ZnX_2, x	Expected Halozincate Complex
$[C_8C_1Im]Cl$	Cl	0.33	2.882	12.49	0.838	6.15	0.33	$[ZnCl_4]^{2-}$
$[P_{6,6,6,14}]Cl$	Cl	0.33	1.986	3.83	0.258	1.893	0.33	$[ZnCl_4]^{2-}$
$[C_8C_1Im]Cl$	Cl	0.50	2.914	12.62	1.722	12.64	0.50	$[Zn_2Cl_6]^{2-}$
$[C_8C_1Im]Cl$	Cl	0.67	2.917	12.64	3.493	25.63	0.67	$[Zn_4Cl_{10}]^{2-}$
$[C_8C_1Im]Br$	Br	0.33	1.919	6.97	0.779	3.46	0.33	$[ZnBr_4]^{2-}$
$[C_8C_1Im]Br$	Br	0.50	2.051	7.45	1.679	7.46	0.50	$[Zn_2Br_6]^{2-}$
$[C_8C_1Im]Br$	Br	0.67	1.953	7.09	3.248	14.42	0.67	$[Zn_2Br_{10}]^{2-}$

The halozincate ionic liquid samples ($\sim$1 drop) were mounted between two pieces of Kapton tape, and were kept in place by a plastic O-ring. We used the Si(111) monochromator crystal cut. VtC measurements were taken using the I20 high-resolution X-ray emission spec-

trometer[44] equipped with three Ge(555) analyser crystals. The spectrometer was calibrated using a Zn foil, measuring the K$\beta_1$and K$\beta_{2,5}$ lines with the incident energy tuned +100 eV from the Zn 1s absorption edge. Further details regarding the stability of the samples under X-ray radiation are provided in the Supporting Information.

Computational Methods

The calculated spectra are based upon the isolated (gas phase) $[Zn_yCl_{2y+2}]^{2-}$ and $[Zn_yBr_{2y+2}]^{2-}$ (where y = 1, 2 and 4) ions optimised at the B3LYP/6-31G* level of theory. The X-ray emission spectra were computed with TDDFT using a protocol described previously.[36] In this approach, a Kohn-Sham DFT calculation is performed for the core-ionised state with the maximum overlap method[45] used to maintain the metal 1s core-hole during the SCF procedure and in a subsequent TDDFT calculation the emission energies appear as negative eigenvalues. The B3LYP exchange-correlation functional was also used for these TDDFT calculations. This functional systematically overestimates the VtC transition energies, and an energy shift is applied to the computed spectra so that the most intense feature aligns with the corresponding band observed in the experiment. These TDDFT calculations are based upon the core-ionised determinant and it has been shown that it is important to use a basis set that is able to describe the core-ionised state.[41,43] In these calculations we adopt the Z+1 basis set procedure wherein the basis set for the core-ionised element is augmented with the basis functions for the element with a nuclear charge that is one higher.[43] The 6-311G* basis set was used for chlorine and bromine, with the (Z+1)6-31G* basis set used for zinc. We emphasise that the same energy shift is applied to all the TDDFT calculations. Spectra are also computed based upon Kohn-Sham DFT calculations using equations 1 and 2. For these calculations the SRC1R1 functional was used,[46] following previous work,[31] with the 6-311G* basis set used for chlorine and bromine, with the 6-31G* basis set used for zinc. These calculations are based upon the ground state Kohn-Sham determinant so the additional basis

7

functions are not required. The calculation of the intensities is performed within the dipole approximation but additional calculations to determine the quadrupole contribution to the intensities have been performed. Relativistic effects are also significant for K-edge X-ray spectroscopy of transition metal elements which lead to a lowering in the energy of the 1s orbital. These effects are accounted for by applying an energy shift to the computed transition energies which is estimated from the difference in the 1s orbital energy between relativistic and non-relativistic HF/cc-pCVQZ for the relevant atom with the relativistic effects modelled using the Douglas-Kroll-Hess Hamiltonian, which gives a value of +88.2 eV for zinc. This calculated shift is insensitive to the binding of different ligands. Calculations of the zinc atom, $ZnCl_4$ and $ZnBr_4$ show a variation of less than 0.04 eV at the HF/cc-pCVTZ level, which compares to a variation of approximately 2 eV between the cc-pCVTZ and cc-pCVQZ basis sets. The advantage of using the single value based upon the zinc atom is that it avoids the need for calculations using large basis sets for the larger clusters. All calculations were performed with the Q-CHEM software package[47] except the calculations to determine the quadupole contribution to the oscillator strengths which were performed using the ORCA software.[48,49] Computational spectra were generated by convoluting the computed energies and oscillator strengths with gaussian functions with full-width at half maximum of 0.25 eV. This value has been chosen to provide a visual representation of the calculated data, and has not been chosen to provide an optimal match with the experimental data.

Results and Discussion

The optimised structures of the complexes are shown in Figure 1, with the bond lengths and bond angles given. $[ZnX_4]^{2-}$, $[Zn_2X_6]^{2-}$ and $[Zn_4X_{10}]^{2-}$ all have four terminal X atoms (i.e. X bonded only to one Zn atom). $[Zn_2X_6]^{2-}$ and $[Zn_4X_{10}]^{2-}$ both have bridged X atoms (i.e. X bonded to two Zn atoms), two and six bridged X atoms respectively; $[ZnX_4]^{2-}$ has only terminal X atoms and no bridged X atoms. $[ZnCl_4]^{2-}$ and $[ZnBr_4]^{2-}$ are tetrahedral with
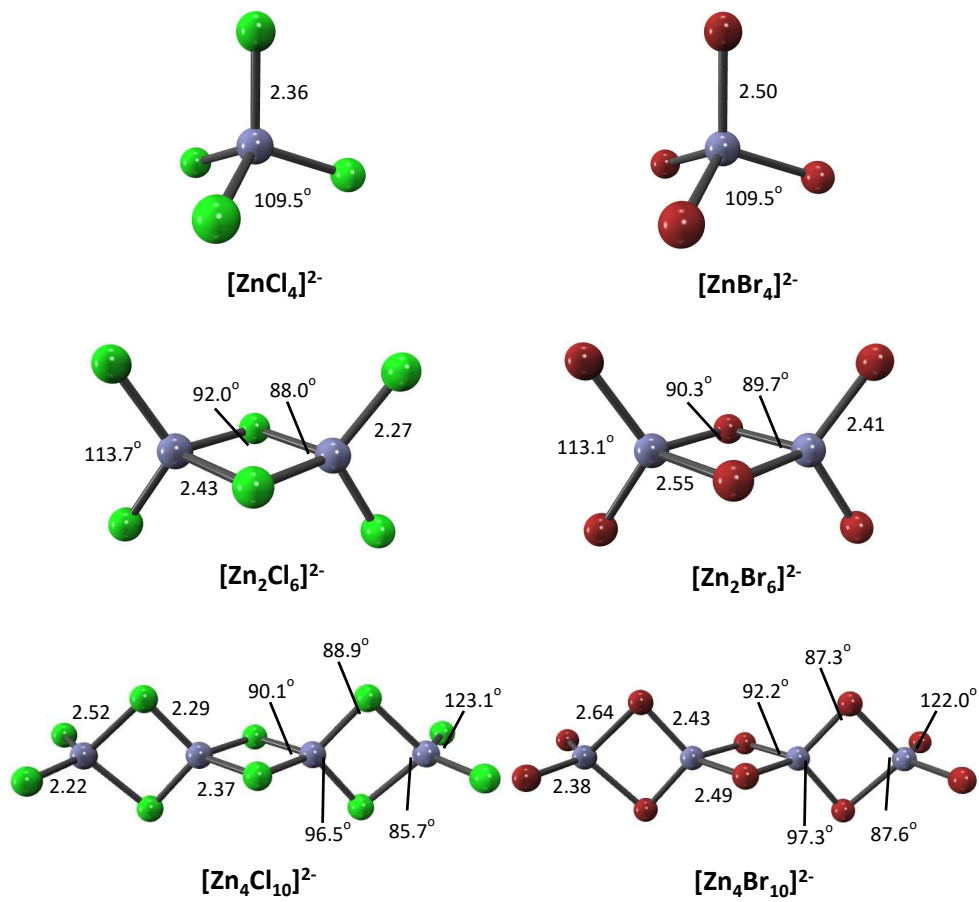
Figure 1: Calculated structures of the isolated $[\text{Zn}_y\text{Cl}_{2y+2}]^{2-}$ and $[\text{Zn}_y\text{Br}_{2y+2}]^{2-}$ ($y = 1$, 2 and 4) ions with bond angles and bond lengths (in Å) shown.

a larger bond length in the bromine complex. The structures of $[Zn_2Cl_6]^{2-}$ and $[Zn_4Cl_{10}]^{2-}$ have a high degree of symmetry and conform to the C_{2v} point group. This has the consequence that the two zinc atoms are equivalent in $[Zn_2Cl_6]^{2-}$, and the two inner and the two outer zinc atoms equivalent in $[Zn_4Cl_{10}]^{2-}$. There is some deviation from the perfect tetrahedral geometry around the zinc atoms, with a narrowing of the Cl–Zn–Cl bond angles for the chlorine atoms bonded to two zinc atoms and a widening of the Cl–Zn–Cl bond angles for the singly bonded chlorine atoms. The bond lengths of the singly bonded chlorine atoms is also shorter. The structures for $[Zn_2Br_6]^{2-}$ and $[Zn_4Br_{10}]^{2-}$ show the same structural trends but with larger bond lengths than the corresponding chlorine complexes.

Figure 2 shows the experimental and calculated TDDFT VtC X-ray emission spectra for $[ZnCl_4]^{2-}$ and $[ZnBr_4]^{2-}$. The intensities of theoretical spectra have been determined within the dipole approximation and to align the calculated spectrum for $[ZnCl_4]^{2-}$ with experiment it is necessary to apply an energy shift of -59.9 eV (in addition to the energy shift to account for relativistic effects). This correction is necessary owing to deficiencies in the exchange-correlation functional,[36] and this shift is subsequently applied to all TDDFT calculated spectra. For $[ZnCl_4]^{2-}$ the experimental spectrum shows four distinct peaks. The highest energy peak at about 9664 eV arises from multi-electron processes which will not be captured by the TDDFT calculations,[17] and this band in not considered further in our analysis. The most intense band lies at 9654.5 eV and the calculations show that this band arises from emission from valence orbitals that have ligand p orbital character, and as a consequence this band can be considered a $K\beta_{2,5}$ line. Therefore, we identify the highest occupied fragment orbital for the halozincate metal complexes as arising from a molecular orbital with ligand p orbital character. In a similar way, the lowest energy band at about 9644 eV arises from orbitals with ligand s orbital character and this band constitutes the $K\beta''$ line. Each of these bands has contributions from three triply degenerate orbitals. In between these two bands the experimental spectrum has a further band at 9649 eV, while
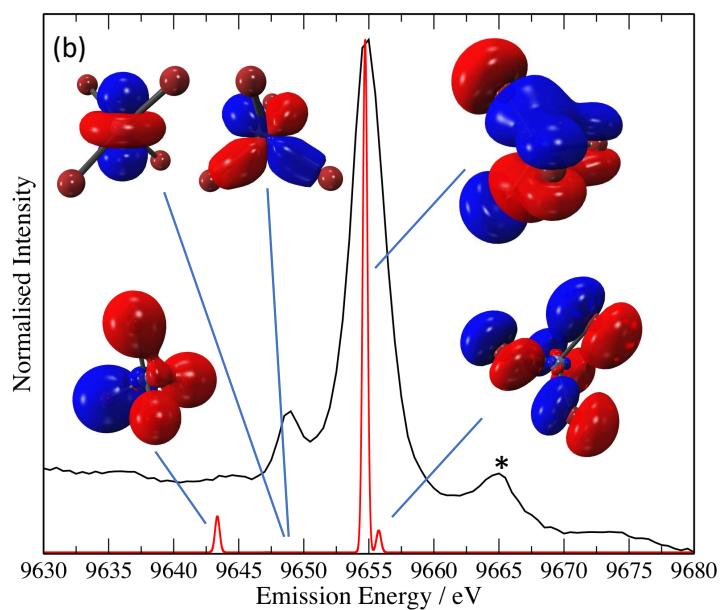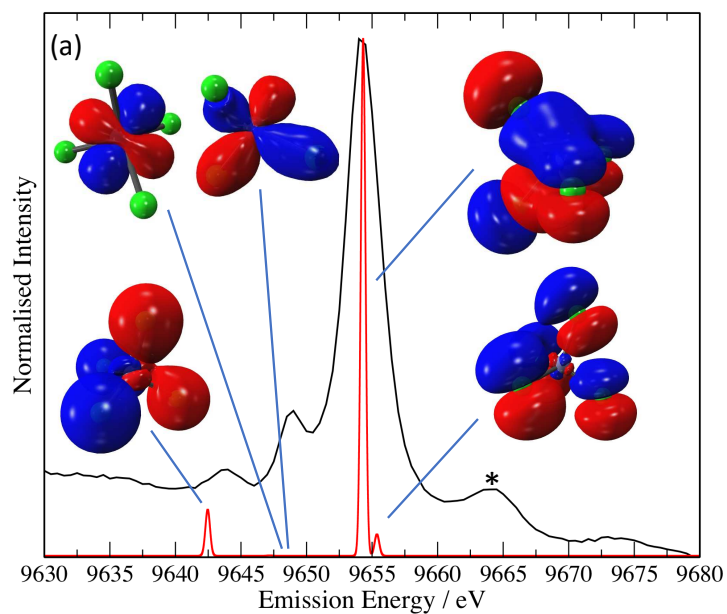
Figure 2: Experimental (black line) and TDDFT (red-line) VtC X-ray emission spectra for (a) $[ZnCl_4]^{2-}$ and (b) $[ZnBr_4]^{2-}$. The intensities of the calculated spectra are determined within the dipole approximation and an energy shift of -59.9 eV is applied. * indicates a multi-electron feature.

11

the calculated spectrum shows no band in this region. Further analysis of the calculated data shows that in this region there lies transitions from the d orbitals of zinc. However, these transitions are predicted to have no intensity owing to the dipole approximation that is used in determining the oscillator strengths, and the calculation of the intensity of this band will be addressed later. The corresponding spectrum for $[ZnBr_4]^{2-}$ is very similar to the $[ZnCl_4]^{2-}$ spectrum (see Figure 2) and the same conclusions can be made.
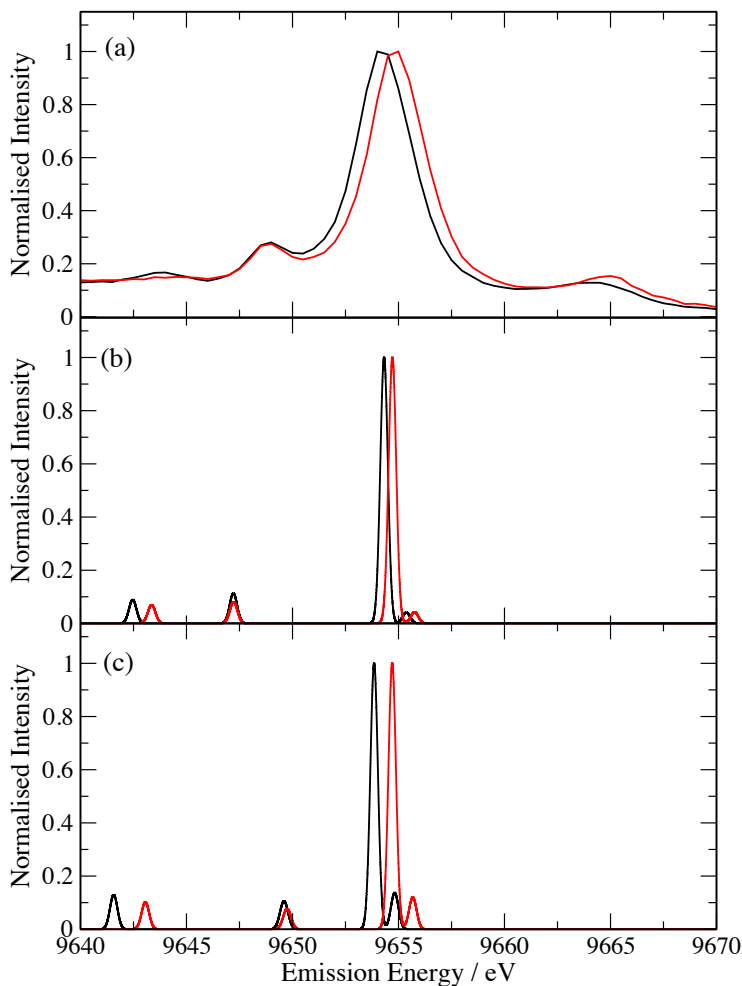

Figure 3: A comparison between the VtC X-ray emission spectra for $[ZnCl_4]^{2-}$ (black line) and $[ZnBr_4]^{2-}$ (red line). (a) experiment, (b) TDDFT and (c) Kohn-Sham DFT. An energy shift of -59.9 eV is applied to the TDDFT spectra and a shift of +4.0 eV is applied to the Kohn-Sham DFT spectra.

In Figure 3 a comparison is made between the VtC emission spectra of $[ZnCl_4]^{2-}$ and

$[ZnBr_4]^{2-}$ from experiment, TDDFT and Kohn-Sham DFT calculations. An energy shift is derived for the Kohn-Sham DFT spectra in an analogous way to TDDFT, giving an energy shift of +4.0 eV. This shift is much smaller because of the different computational approach and the nature of the SRC1R1 functional used.[31] In the calculated spectra the zinc d orbital band has been incorporated by evaluating the intensity of these transitions. To determine these intensities it is necessary to go beyond the dipole approximation and include quadrupole contributions. The ratio of the intensity of the intense band and the zinc d orbital band has been determined using the protocol of Lee *et al.*[4] using DFT calculations. This ratio has been determined for $[ZnCl_4]^{2-}$ and $[ZnBr_4]^{2-}$ and then used to estimate the intensity of the zinc d orbital band in the calculations presented. The inclusion of quadrupole contributions makes a negligible contribution to the dipole allowed transitions, e.g. Zn 1s←ligand p, but do make a significant contribution for the zinc d orbital band. The calculated intensity of the band remains too low compared to the p orbital contributions, relative to the experimental data, but the band can be clearly distinguished in calculated spectra. This shows that to predict all three peaks associated with the single electron transitions it is necessary to go beyond the dipole approximation and include quadrupole contributions. The spectra computed with the Kohn-Sham DFT approach are very similar to the TDDFT spectra consistent with earlier work that found this approach accurate for the simulation of VtC X-ray emission spectra for transition metal complexes.[31] In fact, the energy of the zinc d orbital band aligns more closely with the experiment. Both experimental and calculated XE spectra reveal some subtle differences between the spectra for $[Zn_yCl_{2y+2}]^{2-}$ and $[Zn_yBr_{2y+2}]^{2-}$. For all XE spectra, the band due to the ligand p orbitals was at higher energy by 0.5 eV for $[Zn_yBr_{2y+2}]^{2-}$ compared with $[Zn_yCl_{2y+2}]^{2-}$, irrespective of y. However, for both experiments and calculations the peak with a significant contribution from Zn d orbitals occurred at approximately the same energy for all seven halozincate ionic liquids studied here (see ESI). These findings suggest that each bromozincate ionic liquid will have a smaller ionization energy than the corresponding chlorozincate ionic liquid (for the same y). Furthermore, each

13

bromozincate ionic liquid may be expected to act as a better electron donor (i.e. Lewis base) than the corresponding chlorozincate ionic liquid (again, for the same y). There is also a small reduction in the relative intensity of the low energy band in comparison with the most intense band.
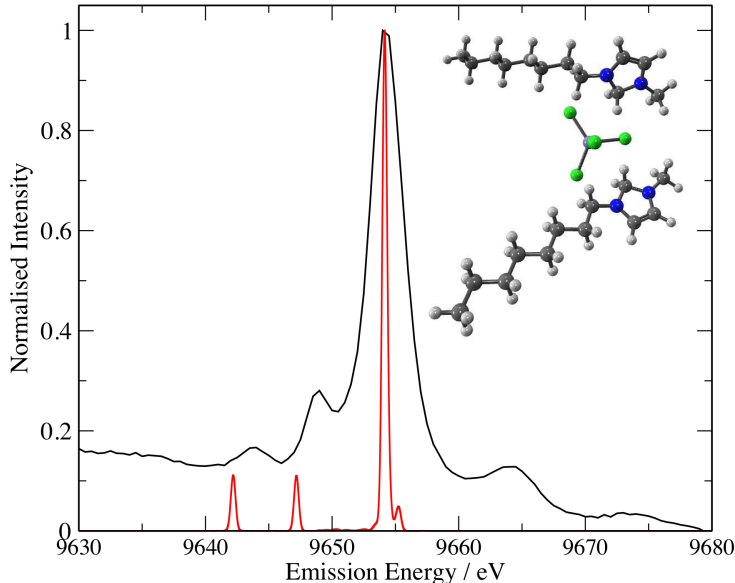

Figure 4: TDDFT calculated VtC X-ray emission spectrum for $[C_8C_1Im]_2[ZnCl_4]$ (red line) and experiment (black line). An energy shift of -59.9 eV is applied to the calculated spectra.

The calculated spectra presented are based upon the isolated metal complex ions whereas the experimental spectra are measured in ionic liquid environment. The ionic liquid environment could potentially have an effect on the VtC emission spectrum. It it is possible to treat the ionic liquid environment at a computationally less expensive molecular mechanics level,[50] however, here we include the counterions explicitly within the calculation. Figure 4 shows the calculated spectra with two $[C_8C_1Im]^+$ ions included explicitly in the calculations, giving an overall neutral species. The results of the calculation indicate that the solvation environment of the metal complex in the ionic liquid does not have a significant effect on the spectrum, and as a consequence modelling the system with a single anion is a good approximation. This is supported by additional measurements of the spectrum with a different

14

countercation (see the supporting information Figure S3a) which show a lack of variation with respect to the identity of the countercation. This is consistent with the view that XES provides a more local probe of electronic structure. In contrast, XAS involves excitation to virtual orbitals which tend to be more diffuse, and it has been shown that calculations of XAS of molecules in ionic liquids requires consideration of at least an ion pair (i.e. one cation and one cation).[51]
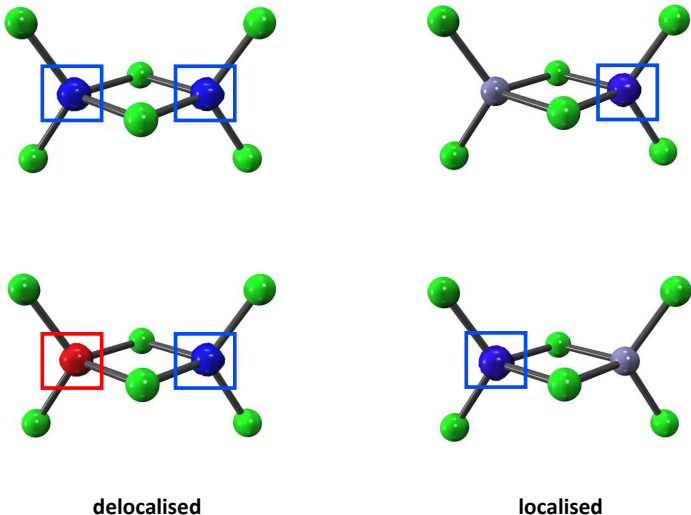

delocalised   **localised**

Figure 5: Delocalised and localised zinc 1s core orbitals of $[Zn_2Cl_6]^{2-}$. The coloured boxes highlight the in-phase and out-of-phase combinations of the Zn 1s orbitals in the delocalised orbitals, in contrast to the localised description where the orbitals have a contribution from a single zinc atom.

We now consider the larger complex $[Zn_2Cl_6]^{2-}$. The optimised structure of this complex has C_{2v} symmetry where the two zinc atoms will be equivalent. In the ground state, the zinc 1s core orbitals will be delocalised over both zinc atoms with in-phase and out-of-phase combinations. In the TDDFT calculations where the core-ionised state is explicitly considered, it is possible to adopt a delocalised or localised representation of the core-hole wherein the core-hole can be on either of the two zinc atoms. The localised representation can be obtained by lowering the symmetry of the wavefunction which allows the core-hole to localise on a single zinc atom. These two representations of the core orbitals are illustrated in Figure 5. The

calculated spectra for core-hole delocalised and core-hole localised reference determinants are shown in Figure 6 along with the experimental spectrum. The calculated spectral profiles for the two states is similar with the only notable difference being a greater intensity of the highest energy band in the core-delocalised spectrum, however, the experimental band is too broad to distinguish between these bands. There is a significant difference in the calculated transition energies, with the local core-hole spectrum aligning closely with experiment while the spectrum for the delocalised core-hole appears at much lower energy. The spectrum for the localised core-hole also aligns closely with the calculated spectrum for $[ZnCl_4]^{2-}$. This is consistent with the experimental measurements that demonstrate clearly that there is no large energy shift between the spectra for $[Zn_2Cl_6]^{2-}$ and $[ZnCl_4]^{2-}$. The delocalised core-hole reference leads to an underestimation of X-ray emission energies which is counter to expectations for the B3LYP functional.[36] Consequently, the comparison between the calculations and experimental data suggests that the localised core-hole description is more appropriate. In the ionic liquid solution, the metal complex would not retain the high symmetry of the gas-phase complex and so a local description of the core-hole would be more appropriate.

Figure 7 shows the experimental and TDDFT spectra for all of the complexes studied. The spectra for the $[Zn_4Cl_{10}]^{2-}$ and $[Zn_4Br_{10}]^{2-}$ complexes were computed based upon two separate calculations, one with the core-hole on an outer zinc atom and one with the core-hole on an inner central zinc atom. The total spectra were then generated by combining the data from the two calculations. The experimental spectra show little variation as the cluster gets larger. There is no change in the position of the bands, but there is a small increase in the intensity of the lower energy bands relative to the band with highest intensity. There is also evidence for a broadening of the intense band which is evident in the calculations and the experimental spectra. These bands lie on the tail of the $K\beta_{1,3}$ emission line and some care needs to be taken in analysing the intensity of these bands. A fuller discussion of this can be found elsewhere.[17] While the spectra cannot clearly distinguish between the
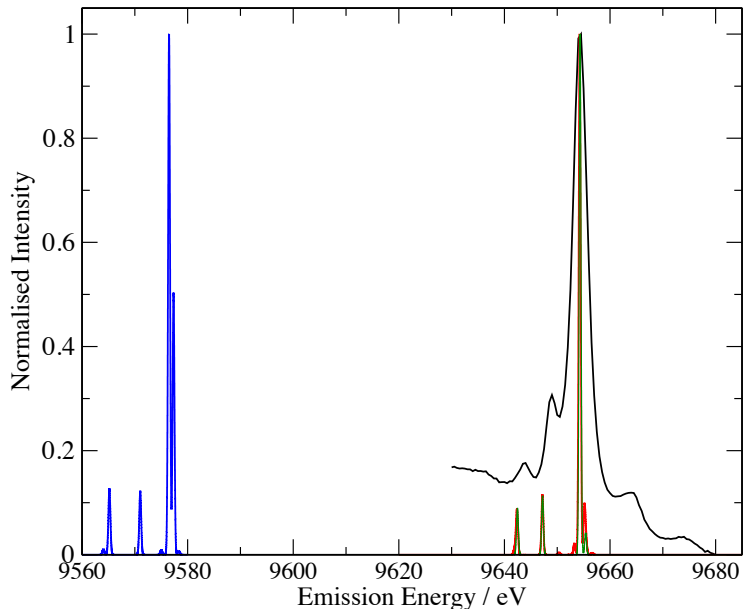
Figure 6: VtC X-ray emission spectra for $[Zn_2Cl_6]^{2-}$. Experiment (black line), TDDFT localised core-hole (red line), TDDFT delocalised core-hole (blue line) and spectrum for $[ZnCl_4]^{2-}$ (green line). An energy shift of -59.9 eV is applied to the calculated spectra.

different sizes of cluster there is an observable energy shift between the chlorine and bromine complexes. The calculations are consistent with this picture and illustrate that the relatively small structural changes in the coordination environment of the zinc atoms do not lead to significant changes in the VtC spectra.

Conclusions

VtC X-ray emission spectra of multi-centre zinc complexes in ionic liquids have been measured and compared with TDDFT calculations. Three distinct bands are observed in the spectra, the most intense band at approximately 9655 eV arises from transitions that have ligand p orbital character, transitions from zinc d orbitals give a band at 9647 eV, while the final band lies at about 9643 eV and arises from emission from orbitals with ligand s character. There is surprisingly little variation between the spectra from $[ZnX_4]^{2-}$, $[Zn_2X_6]^{2-}$
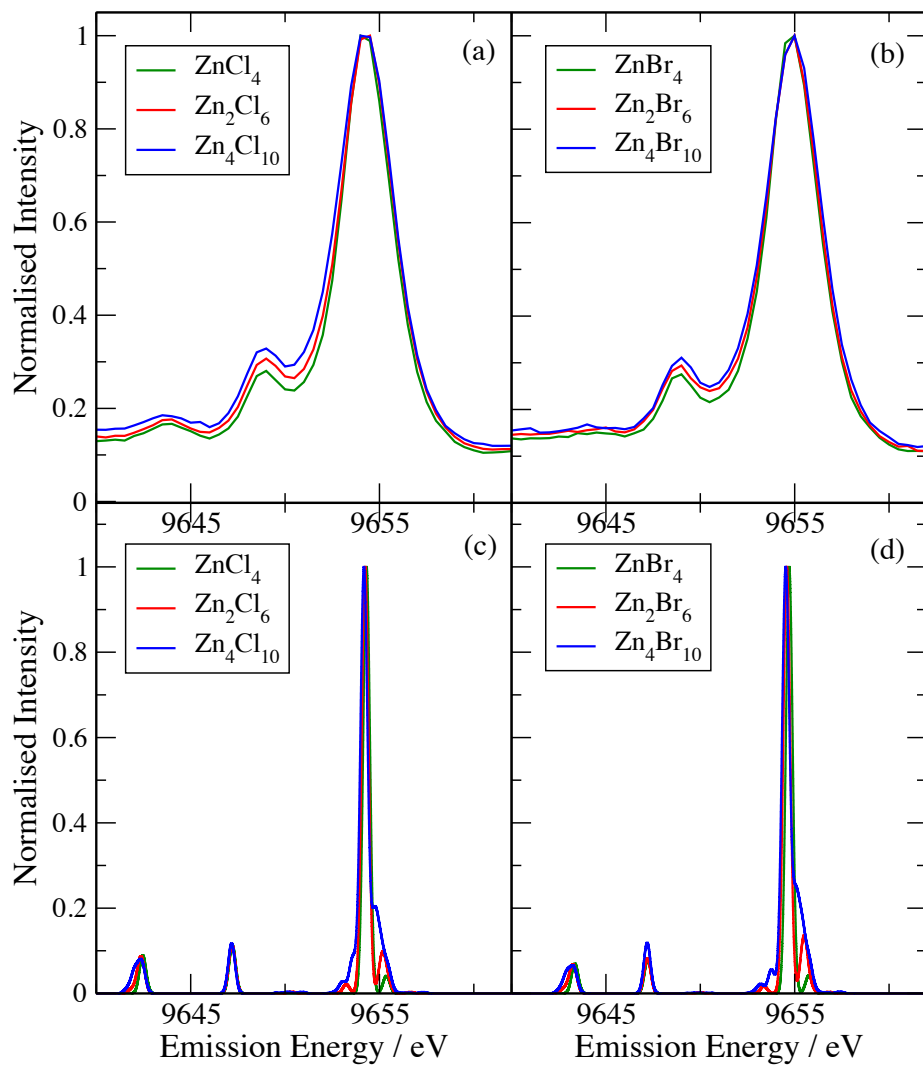
Figure 7: Experimental and TDDFT calculated VtC spectra. (a) experimental spectra for the $[Zn_yCl_{2y+2}]^{2-}$ complexes, (b) experimental spectra for the $[Zn_yBr_{2y+2}]^{2-}$ complexes, (c) calculated spectra for the $[Zn_yCl_{2y+2}]^{2-}$ complexes and (d) calculated spectra for the $[Zn_yBr_{2y+2}]^{2-}$ complexes.

and $[Zn_4X_{10}]^{2-}$ ions, where X=Cl or Br, but there is a shift to higher energy of 0.5 eV for the bromine species. The TDDFT calculations predict three bands in good agreement with the experimental data, but it is necessary to include quadrupole contributions to the oscillator strength for the emission lines associated with transitions from the zinc d orbitals. For the larger ions, the calculations find that the correct reference state has a localised core-hole. In this picture, the spectra can be viewed as a sum of $[ZnX_4]^{2-}$-like spectra with slightly different structures. Since the spectra are relatively insensitive to small changes in the coordination environment, this is consistent with the experimental data that shows little variation in the spectra arising from the different size ions.

Conflicts of Interest

There are no conflicts of interest to declare.

Acknowledgements

Supporting Information

The Supporting Information is available free of charge at the ACS Publications website at DOI:

High resolution Zn 1s NEXAFS spectra monitoring the spectra over time for $[C_8C_1Im]_2[ZnBr_4]$ and $[C_8C_1Im]_2[Zn_4Cl_{10}]$. Zn 1s VtC XE spectra for $[C_8C_1Im]_2[ZnCl_4]$ demonstrating the re-

producibility of the spectra for two different sample mountings. Zn 1s VtC XE spectra for $[C_8C_1Im]_2[ZnCl_4]$ and $[P_{6,6,6,14}]_2[ZnCl_4]$, $[C_8C_1Im]_2[ZnCl_4]$ and $ZnCl_2$ powder. Zn 1s VtC XE spectra for $[C_8C_1Im]_2[ZnCl_4]$, $[C_8C_1Im]_2[ZnBr_4]$ and Zn foil.

References

(1) Nilsson, A.; Pettersson, L. Chemical Bonding on Surfaces Probed by X-Ray Emission Spectroscopy and Density Functional Theory. *Surf. Sci. Rep.* **2004**, *55*, 49–167.

(2) Chen, L. X.; Zhang, X.; Shelby, M. L. Recent Advances on Ultrafast X-Ray Spectroscopy in the Chemical Sciences. *Chem. Sci.* **2014**, *5*, 4136–4152.

(3) Chergui, M.; Collet, E. Photoinduced Structural Dynamics of Molecular Systems Mapped by Time-Resolved X-Ray Methods. *Chem. Rev.* **2017**, *117*, 11025–11065.

(4) Lee, N.; Petrenko, T.; Bergmann, U.; Neese, F.; DeBeer, S. Probing Valence Orbital Composition With Iron Kβ X-Ray Emission Spectroscopy. *J. Am. Chem. Soc.* **2010**, *132*, 9715–9727.

(5) Pollock, C. J.; DeBeer, S. Valence-to-Core X-Ray Emission Spectroscopy: A Sensitive Probe of the Nature of a Bound Ligand. *J. Am. Chem. Soc.* **2011**, *133*, 5594–5601.

(6) Smolentsev, G.; Soldatov, A. V.; Messinger, J.; Merz, K.; Weyhermueller, T.; Bergmann, U.; Pushkar, Y.; Yano, J.; Yachandra, V. K.; Glatzel, P. X-Ray Emission Spectroscopy to Study Ligand Valence Orbitals in Mn Coordination Complexes. *J. Am. Chem. Soc.* **2009**, *131*, 13161–13167.

(7) Beckwith, M. A.; Roemelt, M.; Collomb, M.-N.; DuBoc, C.; Weng, T.-C.; Bergmann, U.; Glatzel, P.; Neese, F.; DeBeer, S. Manganese Kβ X-Ray Emission Spectroscopy as a Probe of Metal-Ligand Interactions. *Inorg. Chem.* **2011**, *50*, 8397–8409.

(8) Delgado-Jaime, M. U.; Dible, B. R.; Chiang, K. P.; Brennessel, W. W.; Bergmann, U.; Holland, P. L.; DeBeer, S. Identification of a Single Light Atom Within a Multinuclear Metal Cluster Using Valence-to-Core X-Ray Emission Spectroscopy. *Inorg. Chem.* **2011**, *50*, 10709–10717.

(9) Lassalle-Kaiser, B.; Boron, T. T.; Krewald, V.; Kern, J.; Beckwith, M. A.; Delgado-Jaime, M. U.; Schroeder, H.; Alonso-Mori, R.; Nordlund, D.; Weng, T.-C; et. al., Experimental and Computational X-Ray Emission Spectroscopy as a Direct Probe of Protonation States in Oxo-Bridged MnIV Dimers Relevant to Redox-Active Metalloproteins. *Inorg. Chem.* **2013**, *52*, 12915–12922.

(10) Atkins, A. J.; Bauer, M.; Jacob, C. R. The Chemical Sensitivity of X-Ray Spectroscopy: High Energy Resolution XANES Versus X-Ray Emission Spectroscopy of Substituted Ferrocenes. *Phys. Chem. Chem. Phys.* **2013**, *15*, 8095–8105.

(11) Pollock, C. J.; Lancaster, K. M.; Finkelstein, K. D.; DeBeer, S. Study of Iron Dimers Reveals Angular Dependence of Valence-to-Core X-Ray Emission Spectra. *Inorg. Chem.* **2014**, *53*, 10378–10385.

(12) Hall, E. R.; Pollock, C. J.; Bendix, J.; Collins, T. J.; Glatzel, P.; DeBeer, S. Valence-to-Core-Detected X-Ray Absorption Spectroscopy: Targeting Ligand Selectivity. *J. Am. Chem. Soc.* **2014**, *136*, 10076–10084.

(13) MacMillan, S. N.; Walroth, R. C.; Perry, D. M.; Morsing, T. J.; Lancaster, K. M. Ligand-Sensitive but Not Ligand-Diagnostic: Evaluating Cr Valence-to-Core X-Ray Emission Spectroscopy as a Probe of Inner-Sphere Coordination. *Inorg. Chem.* **2015**, *54*, 205–214.

(14) Pollock, C. J.; DeBeer, S. Insights into the Geometric and Electronic Structure of Transition Metal Centers From Valence-to-Core X-Ray Emission Spectroscopy. *Acc. Chem. Res.* **2015**, *48*, 2967–2975.

(15) March, A. M.; Assefa, T. A.; Bressler, C.; Doumy, G.; Galler, A.; Gawelda, W.; Kanter, E. P.; Nemeth, Z.; Papai, M.; Southworth, S. H.; et al., Feasibility of Valence-to-Core X-Ray Emission Spectroscopy for Tracking Transient Species. *J. Phys. Chem. C* **2015**, *119*, 14571–14578.

(16) Rees, J. A.; Wandzilak, A.; Maganas, D.; Wurster, N. I. C.; Hugenbruch, S.; Kowalska, J. K.; Pollock, C. J.; Lima, F. A.; Finkelstein, K. D.; DeBeer, S. Experimental and Theoretical Correlations Between Vanadium K-Edge X-Ray Absorption and K Emission Spectra. *J. Bio. Inorg. Chem.* **2016**, *21*, 793–805.

(17) Mortensen, D. R.; Seidler, G. T.; Kas, J. J.; Govind, N.; Schwartz, C. P.; Pemmaraju, S.; Prendergast, D. G. Benchmark Results and Theoretical Treatments for Valence-to-Core X-ray Emission Spectroscopy in Transition Metal Compounds. *Phys. Rev. B* **2017**, *96*, 125136.

(18) Lancaster, K. M.; Roemelt, M.; Ettenhuber, P.; Hu, Y.; Ribbe, M. W.; Neese, F.; Bergmann, U.; DeBeer, S. X-Ray Emission Spectroscopy Evidences a Central Carbon in the Nitrogenase Iron-Molybdenum Cofactor. *Science* **2011**, *334*, 974–977.

(19) Calderon Morales, R.; Tambyrajah, V.; Jenkins, P. R.; Davies, D. L.; Abbott, A. P. The Regiospecific Fischer Indole Reaction in Choline Chloride.$2ZnCl_2$ With Product Isolation by Direct Sublimation From the Ionic Liquid. *Chem. Commun.* **2004**, 158–159.

(20) Abbott, A. P.; Bell, T. J.; Handa, S.; Stoddart, B. O-Acetylation of Cellulose and Monosaccharides Using a Zinc Based Ionic Liquid. *Green Chem.* **2005**, *7*, 705–707.

(21) Duan, Z.; Gu, Y.; Deng, Y. Green and Moisture-Stable Lewis Acidic Ionic Liquids (Choline Chloride.$ZnCl_2$) Catalyzed Protection of Carbonyls at Room Temperature Under Solvent-Free Conditions. *Catal. Commun.* **2006**, *7*, 651–656.

(22) Estager, J.; Nockemann, P.; Seddon, K. R.; Swadźba-Kwaśny, M.; Tyrrell, S. Validation of Speciation Techniques: A study of Chlorozincate(II) Ionic Liquids. *Inorg. Chem.* **2011**, *50*, 5258–5271.

(23) Estager, J.; Holbrey, J. D.; Swadźba-Kwaśny, M. Halometallate Ionic Liquids - Revisited. *Chem. Soc. Rev.* **2014**, *43*, 847–886.

(24) Taylor, A. W.; Men, S.; Clarke, C. J.; Licence, P. Acidity and Basicity of Halometallate-Based Ionic Liquids From X-Ray Photoelectron Spectroscopy. *RSC Adv.* **2013**, *3*, 9436–9445.

(25) Swadźba-Kwaśny, M. Comment on, Lewis Acidic Ionic Liquids of Crown Ether Complex Cations: Preparation and Applications in Organic Reactions, by Y. Liang, J. Wang, C. Cheng and H. Jing, RSC Adv., 2016, 6, 93546. *RSC Adv.* **2017**, *7*, 51907–51909.

(26) Agren, H.; Nordgren, J. Ab Initio Hartree-Fock Calculations of Molecular X-Ray Intensities - Validity of One-Center Approximations. *Theor. Chim. Acta* **1981**, *58*, 111–119.

(27) Agren, H.; Arnberg, R.; Muller, J.; Manne, R. X-Ray-Emission of the Nitrogen Molecule Following Photon or Electron-Impact - A Theoretical-Study Using Configurational Interaction Wavefunctions. *Chem. Phys.* **1984**, *83*, 53–67.

(28) Agren, H.; Floresriveros, A.; Jensen, H. An Efficient Method for Calculating Molecular Radiative Derivatives in the VUV and Soft-X-Ray Wavelength Regions. *Physica Scripta* **1989**, *40*, 745–750.

(29) Florersriveros, A.; Agren, H. Calculations of X-Ray Fluorescence of CO and CO_2. *Physica Scripta* **1991**, *44*, 442–445.

(30) Lee, N.; Petrenko, T.; Bergmann, U.; Neese, F.; DeBeer, S. Probing Valence Orbital Composition With Iron Kβ X-Ray Emission Spectroscopy. *J. Am. Chem. Soc.* **2010**, *132*, 9715–9727.

(31) Hanson-Heine, M. W. D.; George, M. W.; Besley, N. A. Kohn-Sham Density Functional Theory Calculations of Non-Resonant and Resonant X-Ray Emission Spectroscopy. *J. Chem. Phys.* **2017**, *146*, 094106.

(32) Triguero, L.; Pettersson, L.; Agren, H. Calculations of X-Ray Emission Spectra of Molecules and Surface Adsorbates by Means of Density Functional Theory. *J. Phys. Chem. A* **1998**, *102*, 10599–10607.

(33) Besley, N. A.; Gilbert, A. T. B.; Gill, P. M. W. Self-Consistent-Field Calculations of Core Excited States. *J. Chem. Phys.* **2009**, *130*, 124308.

(34) Besley, N. A.; Asmuruf, F. A. Time-Dependent Density Functional Theory Calculations of the Spectroscopy of Core Electrons. *Phys. Chem. Chem. Phys.* **2010**, *12*, 12024–12039.

(35) Besley, N. A. Equation of Motion Coupled Cluster Theory Calculations of the X-Ray Emission Spectroscopy of Water. *Chem. Phys. Lett.* **2012**, *542*, 42 – 46.

(36) Wadey, J. D.; Besley, N. A. Quantum Chemical Calculations of X-Ray Emission Spectroscopy. *J. Chem. Theory Comput.* **2014**, *10*, 4557–4564.

(37) Zhovtobriukh, I.; Besley, N. A.; Fransson, T.; Nilsson, A.; Pettersson, L. G. M. Relationship Between X-Ray Emission and Absorption Spectroscopy and the Local H-Bond Environment in Water. *J. Chem. Phys.* **2018**, *148*, 144507.

(38) Fransson, T.; Dreuw, A. Simulating X-Ray Emission Spectroscopy With Algebraic Diagrammatic Construction Schemes for the Polarization Propagator. *J. Chem. Theory Comput.* **2019**, *15*, 546–556.

(39) Zhang, Y.; Mukamel, S.; Khalil, M.; Govind, N. Simulating Valence-to-Core X-Ray Emission Spectroscopy of Transition Metal Complexes With Time-Dependent Density Functional Theory. *J, Chem. Theory Comp.* **2015**, *11*, 5804–5809.

(40) Roper, I. P.; Besley, N. A. The Effect of Basis Set and Exchange-Correlation Functional on Time-Dependent Density Functional Theory Calculations Within the Tamm-Dancoff Approximation of the x-Ray Emission Spectroscopy of Transition Metal Complexes. *J. Chem. Phys.* **2016**, *144*, 114104.

(41) Fouda, A. E. A.; Besley, N. A. Assessment of Basis Sets for Density Functional Theory-Based Calculations of Core-Electron Spectroscopies. *Theor. Chem. Acc.* **2017**, *137*, 6.

(42) Ambroise, M. A.; Jensen, F. Probing Basis Set Requirements for Calculating Core Ionization and Core Excitation Spectroscopy by the Δ Self-Consistent-Field Approach. *J. Chem. Theory Comput.* **2019**, *15*, 325–337.

(43) Hanson-Heine, M. W.; George, M. W.; Besley, N. A. Basis Sets for the Calculation of Core-Electron Binding Energies. *Chem. Phys. Lett.* **2018**, *699*, 279 – 285.

(44) Diaz-Moreno, S.; Amboage, M.; Basham, M.; Boada, R.; Bricknell, N. E.; Cibin, G.; Cobb, T. M.; Filik, J.; Freeman, A.; Geraki, K.; et al., The Spectroscopy Village at Diamond Light Source. *J. Synchrotron Radiat* **2018**, *25*, 998–1009.

(45) Gilbert, A. T. B.; Besley, N. A.; Gill, P. M. W. Self-Consistent Field Calculations of Excited States Using the Maximum Overlap Method (MOM). *J. Phys. Chem. A* **2008**, *112*, 13164–13171.

(46) Besley, N. A.; Peach, M. J. G.; Tozer, D. J. Time-Dependent Density Functional Theory Calculations of Near-Edge X-Ray Absorption Fine Structure With Short-Range Corrected Functionals. *Phys. Chem. Chem. Phys.* **2009**, *11*, 10350–10358.

(47) Shao, Y.; Gan, Z.; Epifanovsky, E.; Gilbert, A. T.; Wormit, M.; Kussmann, J.; Lange, A. W.; Behn, A.; Deng, J.; Feng, X.; et al., Advances in Molecular Quantum Chemistry Contained in the Q-Chem 4 Program Package. *Mol. Phys.* **2015**, *113*, 184–215.

(48) Neese, F. The ORCA Program System. *Wiley Interdisciplinary Reviews: Computational Molecular Science* **2012**, *2*, 73–78.

(49) Neese, F. Software Update: The ORCA Program System, Version 4.0. *Wiley Interdisciplinary Reviews: Computational Molecular Science* **2018**, *8*, e1327.

(50) Briggs, E. A.; Besley, N. A.; Robinson, D. QM/MM Excited State Molecular Dynamics and Fluorescence Spectroscopy of BODIPY. **2013**, *117*, 2644–2650.

(51) Fogarty, R. M.; Matthews, R. P.; Clough, M. T.; Ashworth, C. R.; Brandt-Talbot, A.; Corbett, P. J.; Palgrave, R. G.; Bourne, R. A.; Chamberlain, T. W.; Vander Hooger- straete, T.; et al., NEXAFS Spectroscopy of Ionic Liquids: Experiments Versus Calculations. *Phys. Chem. Chem. Phys.* **2017**, *19*, 31156–31167.

Table of Contents Graphic